[논 문] 한국재료학회지
Kor. J. Mater. Res.
Vol. 17, No. 2 (2007)

Effect of $MgO-P_2O_5$ Sintering Additive on Microstructure of Sintered Hydroxyapatite (HAp) Bodies and Their In-Vitro Study

Byong-Taek Lee*, Hyeong-Chul Youn*, Chi-Woo Lee* and Ho-Yeon Song†

Department of Microbiology, School of Medicine, Soonchunhyang University, 366-1, Ssangyoung-dong, Cheonan, Chungnam 330-090 Korea
*School of Advanced Materials Engineering, Kongju National University, 182, Shinkwan-dong, Kongju, Chungnam 314-701 Korea

(2007년 2월 9일 받음, 2007년 2월 20일 최종수정본 받음)

Abstract The effects of $MgO-P_2O_5$ based sintering additive on the microstructure and material and biological properties of hydroxyapatite (HAp, $Ca_{10}(PO_4)_6(OH)_2$) ceramic were investigated using XRD, SEM and TEM techniques. The $MgO-P_2O_5$ sintering additive improved the material properties and increased the grain size in the sintered HAp bodies. As the content of sintering additive increased over 4 wt%, a small amount of the HAp phase was decomposed and transformed to β-TCP. In the 2 wt% $MgO-P_2O_5$ content HAp sintered body, the maximum values of density and hardness were respectively about 3.10 gm/cc and 657 HV. However, the maximum fracture toughness in the HAp body containing 8 wt% $MgO-P_2O_5$ was about 1.02 $MPa \cdot m^{1/2}$ due to the crack deflection effect. Human osteoblast like MG-63 cells and osteoclast like raw 264.7 cells were well grown and fully covered all of the HAp sintered bodies. The osteoblast cells were grown with spindle-shaped and the osteoclast cells had a grape-like round shape.

Key words Hydroxyapatite, Sintering additive, $MgO-P_2O_5$, Microstructure, In-vitro study.

1. Introduction

For the application of biomaterials in the human body, they must simultaneously satisfy many requirements such as non-toxicity, corrosion resistance, thermal conductivity, strength, fatigue durability, biocompatibility and sometimes aesthetics.[1,2] Among the biomaterials, calcium phosphate-based ceramics have been receiving much attention as potential bone substitutes because of their biocompatibility, bioactivity and osteoconduction characteristics.[3,4] The first successful medical application of calcium phosphate reagent was reported for the repair of bone defect in humans as well as dental application in animals.[5] The most widely used calcium phosphate based bioceramics are Hydroxyapatite (HAp, $Ca_{10}(PO_4)_6(OH)_2$), dicalcium phosphate ($CaHPO_4 \cdot 2H_2O$) and â-tricalcium phosphate (β-TCP, $Ca_3(PO_4)_2$). Among them, HAp and dicalcium phosphate are stable in the human body and in the body fluid at pH >4.2 and pH <4.2, respectively. It is well known that the pH of human blood is about 7.3.[6] Therefore, the dense HAp has been recognized for applications of bioimplants such as the repair of bone defects in dental and orthopaedic implants and tooth root replacements etc.[7-10] However, its application has been limited to load bearing parts due to its inherent lower mechanical properties compared to other bioinert ceramics such as alumina and zirconia.[11,12] Therefore, many researchers have been focused on improving the mechanical properties by the optimization of processing conditions and sintering additives. Among them the liquid phase sintering has been recognized as a highly potential route[13] and investigated using the addition of CaO, P_2O_5, MgO, Na_2O or their combination. In the HAp sintered bodies using P_2O_5 and $CaO-P_2O_5$ based sintering additive, the flexural strength was increased compared with monolithic HAp sintered bodies.[14] However, there was no study using of $MgO-P_2O_5$ binary oxide system for the densification of HAp sintered bodies.

In this study, $MgO-P_2O_5$ system was used as a sintering additive to enhance the material properties of HAp sintered bodies without changing their biocompatibility. Especially, their microstructure and material properties depending on the content of $MgO-P_2O_5$ were investigated using XRD, SEM and TEM techniques. In addition, the biocompatibility was investigated using the osteoblast like human MG-63 and osteoclast raw 264.7 cells.

†Corresponding author
E-Mail : songmic@sch.ac.kr (H.-Y. Song)

2. Experiment procedure

Hyderoxyapatite (HAp, $Ca_{10}(PO_4)_6(OH)_2$), (Strem Chemicals, Newburyport, MA 01950 USA), Magnesium Oxide (MgO, Alfa Aesar) and Phosphorous Pentoxide (P_2O_5, Samchun Pure Chemical Co. Ltd, Korea) were used as starting materials. First, MgO and P_2O_5 powders with a volume ratio of about 60:40 were homogeneously mixed using the ball mill. Then, the mixing powders were crushed and ground into fine powders using a mortar and pestle. Second, HAp powder was mixed with small quantities (0, 1, 2, 3, 4, 6 and 8 wt.%) of as-prepared $MgO-P_2O_5$ additive in ethanol by ball mill for 20 hrs using Al_2O_3 balls as milling media. After mixing, the milling media was separated and dried on a hot plate while stirring. The dried powders of variant compositions were compacted by a uniaxial compaction machine into pellets. The green pellets were sintered at 1200°C for 2 hrs in an air atmosphere.

The morphology, crystal structure and internal microstructures of monolithic HAp and $MgO-P_2O_5$ content HAp sintered bodies were identified using SEM (JSM-635F, Jeol, Japan), XRD (DMAX 250, Rigaku, Japan) and TEM (JEM-2010, JEOL, Japan), respectively. Densities of the sintered samples were measured by the Archimedes method with an immersion medium of water. The Vickers hardness (HV-112, Akashi, Japan) was measured using 2.5 kg load and the fracture toughness was calculated by the indentation method and Evans equation using 2.5 kg load.

To investigate the adherence and proliferation of cells on the HAp, HAp-4 wt.% and HAp-8 wt.% $MgO-P_2O_5$ content sintered bodies, MG-63 human osteoblast-like cells and osteoclast raw 264.7 cells were used. The cells were maintained in Dulbecco's modification of Eagle's MEM (DMEM, Gibco) containing 10% heat inactivated fetal bovine serum (FBS, Gibco), 2 mM L-glutamine, 100 U/ml penicillin, 100 μg/ml streptomycin and 0.25 μg/ml fungizone (Bio-Whittaker), and were placed in an incubator containing 5% CO_2 at 37°C. A 100 μl of MG-63 cells (5×10^4 cells/ml) were seeded on the top surfaces of HAp, HAp-4 wt.% and HAp-8 wt.% $MgO-P_2O_5$ content sintered bodies (11 mm diameter and 3 mm height) in a 6-well plate. After 5 hrs, the sintered body adhered cells were cultured in new 6-well plates. The growth behaviors of cells were observed after 5 days using a scanning electron microscope (SEM).

3. Results and Discussion

Fig. 1 shows SEM micrographs of HAp sintered bodies depending on the content of $MgO-P_2O_5$ sintering additive. In monolithic HAp sintered bodies as seen in Fig. 1(a), fine

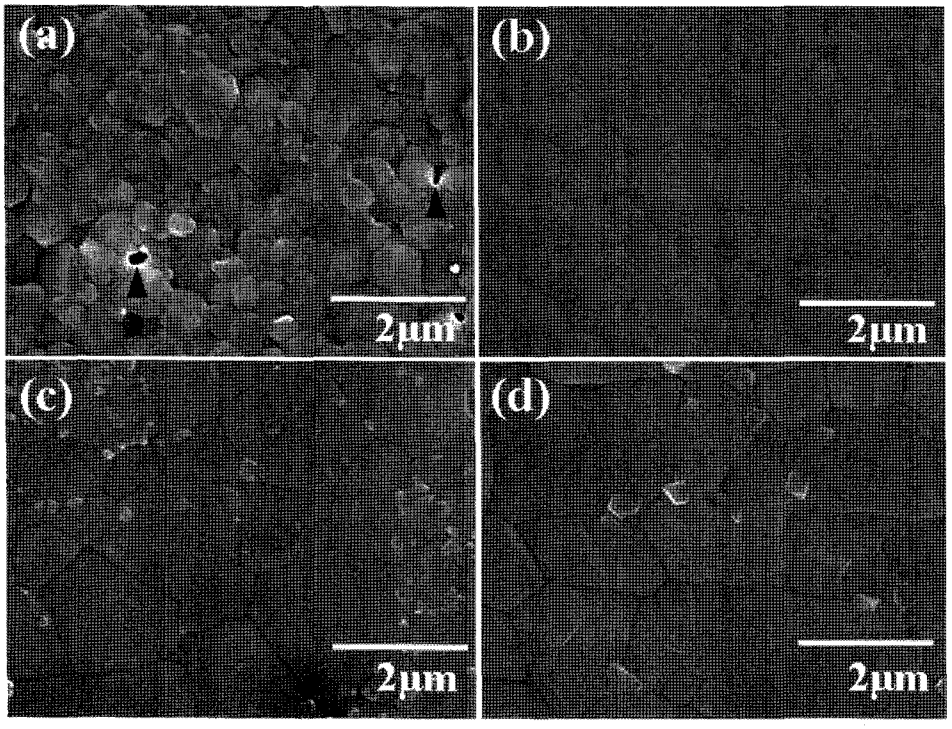

Fig. 1. SEM micrographs of HAp sintered bodies depending on $MgO-P_2O_5$ content; (a) 0 wt.% (b) 2 wt.%, (c) 6 wt.% and (d) 8 wt.%.

grains less than 0.7 μm in diameter were clearly observed as well as a few pores found as indicated with arrowheads. However, as the content of MgO-P_2O_5 increased, grain size increased significantly as shown in Fig. 1(b-d). The average grain size of the HAp sintered body, which contained 2 wt% MgO-P_2O_5, was about 1 μm in diameter. On the other hand, the average grain size in the 6 and 8 wt.% MgO-P_2O_5 content samples were about 1.7 and 2 μm in diameter, respectively. Furthermore, in Fig. 1(c) and (d), a few fine particles were observed with different contrast.

Fig. 2 shows XRD profiles of HAp sintered bodies which contained (a) 0 wt.%, (b) 2 wt.%, (c) 4 wt.%, (d) 6 wt.% and (e) 8 wt.% MgO-P_2O_5. In the low content of MgO-P_2O_5 (a-c), only HAp phase was detected. However, in the sample containing 6 wt.% and 8 wt.% MgO-P_2O_5, β-TCP peaks were also detected although the main peaks were HAp phase. This result indicated that the existence of a liquid phase such as some MgO-P_2O_5 may enhance the transformation of HAp to β-TCP phase. However, in the sample contained 8 wt.% MgO-P_2O_5 (d), some $Ca_4Mg_5(PO_4)_6$ peaks also detected as a minor phase.

Fig. 3 shows TEM micrographs and EDS profiles of HAp sintered bodies which containing 8 wt.% MgO-P_2O_5. Some fine particles less than 0.5 μm in diameter was observed at intra and intergranular type. In the enlarged image shown in Fig. 3(b), some dislocations were also detected in the

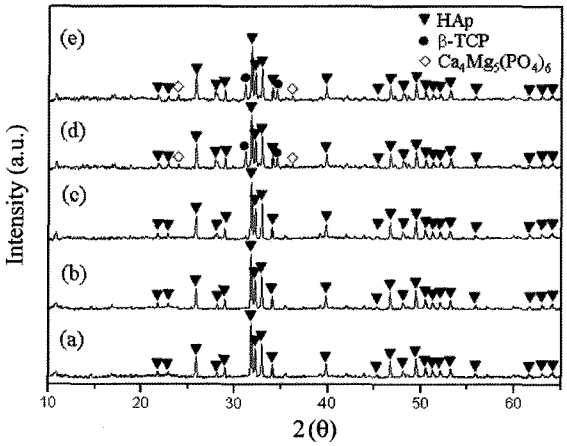

Fig. 2. XRD profiles of HAp sintered bodies depending on MgO-P_2O_5 content; (a) 0 wt.%, (b) 2 wt.%, (c) 4 wt.%, (d) 6 wt.% and (e) 8 wt.%.

HAp grains as indicated by an arrowhead. The formation of dislocations may be due to the mismatch of thermal expansion and lattice parameters. For the detailed analysis of local phases, EDS profiles were taken from 4 regions that were a triple region (marked P), intergranular regions (marked Q, R) and white particles (marked S). As shown in Fig. 3(c), the triple region and intergranular regions were comprised with Ca, P, and O as main elements, but the Mg peak was also detected with very low intensity. However, in the white particles region, the main peak was Mg element

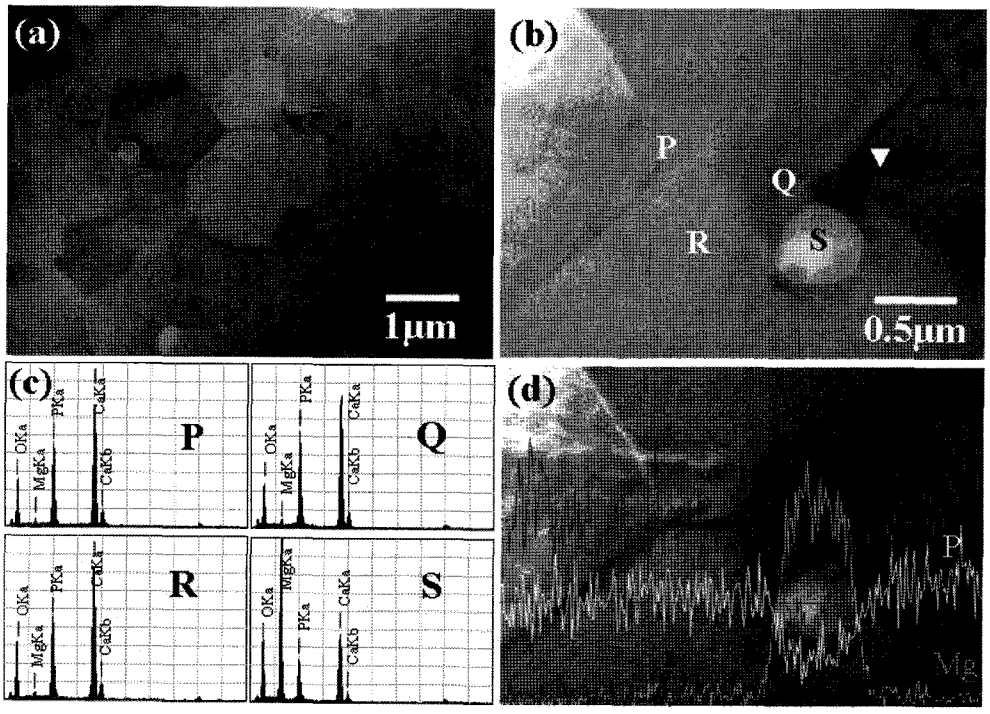

Fig. 3. TEM micrographs (a,b) and EDS profiles (c,d) of HAp- 8 wt.% MgO-P_2O_5 content sintered body.

although Ca, P and O elements were detected. From the line analysis (Fig. 3(d)), it was confirmed that the white particles were Mg rich Ca-P-O compound.

To clearly understand the fracture behavior, crack propagation made by Vickers indentation was observed by SEM. Fig. 4 shows the crack propagation of HAp sintered bodies which contained (a) 2 wt.% and (c) 8 wt.% $MgO-P_2O_5$. The indentation cracks which were made on the polished surface of HAp sintered bodies showed different propagation mode; i.e, in the sample which contained 2 wt.% $MgO-P_2O_5$, a long, typical median crack propagated from four corners of an indentation site, was clearly observed, but in the 8 wt.% $MgO-P_2O_5$ content HAp sintered body, some lateral cracks were found as indicated with an arrowhead in Fig. 4(c), as well as a median crack. The enlarged images shown in Fig. 4(b, d) were taken from the crack propagation zone of each rectangular region in Fig. 4(a) and (c), respectively. In the case of Fig. 4(b), the intergranular crack was relatively straight without any deflection, which frequently appeared in the monolithic HAp sintered body. However, in the sample containing 8 wt.% $MgO-P_2O_5$ in Fig. 4(d), the crack is propagated along the intra and intergranular type with deflection phenomena. This observation means that when the crack propagated into the HAp body containing 8 wt.% $MgO-P_2O_5$, the crack propagation energy can be reduced.

Fig. 5 shows the material properties of HAp sintered bodies depending on the $MgO-P_2O_5$ content. In the monolithic HAp sintered bodies, the material properties such as density, hardness and fracture toughness were about 2.83 gm/cc, 425 Hv and 0.87 MPa · $m^{1/2}$ respectively, which were comparatively lower than those of other samples containing $MgO-P_2O_5$. However, as the sintering additive increased up to 2 wt.%, the density and Vickers hardness values were increased remarkably due to the densification and fine microstructure as shown in Fig. 1(b). Thus, the maximum values of the density and Vickers hardness were about 3.10 gm/cc and 657 Hv, respectively. But, after increasing the sintering additives from 2-8 wt.%, the density gradually

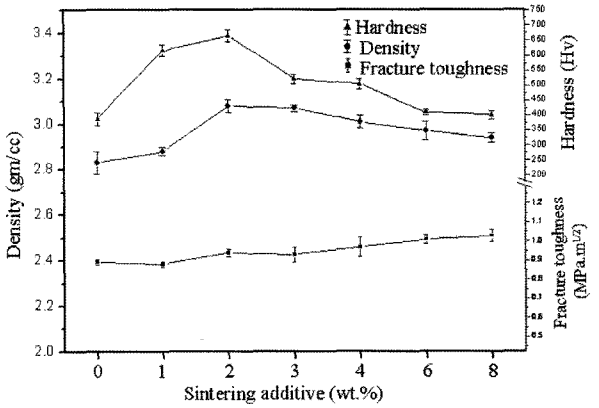

Fig. 5. Material properties of HAp sintered bodies depending on $MgO-P_2O_5$ content.

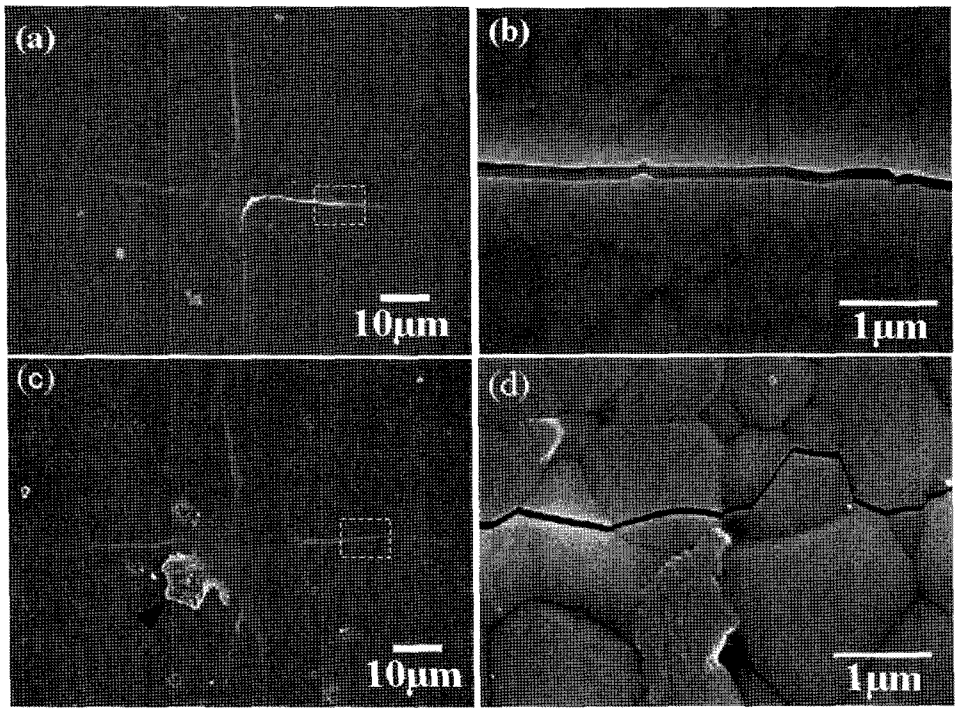

Fig. 4. Crack propagation of HAp sintered bodies depending on $MgO-P_2O_5$ content; (a,b) 2 wt.% and (c,d) 8 wt.%.

decreased. Furthermore, the hardness also decreased due to the decrease in density and grain growth to about 2 μm in diameter. Moreover, the fracture toughness values were not significantly improved due to the absence of a strong toughening mechanism. But, in case of 8 wt.% MgO-P_2O_5 content sample, the fracture toughness value was slightly increased to about 1.02 Map·$m^{1/2}$. The transformation of HAp to β-TCP phases is accompanied by volume change,[12] which creates residual stresses at their grain boundaries. In this case, some microcracking or crack deflection mechanisms can be introduced depending on the stress level. Thus, the reason for the slight increase in the fracture toughness may be due to the crack deflection mechanism. It should also be mentioned that the addition of sintering additive does not significantly increase the fracture toughness of HAp sintered bodies due to the absence of multi-toughening mechanisms.

Fig. 6 shows the SEM fracture surfaces of HAp sintered bodies which contained (a) 0 wt.% and (b) 8 wt.% MgO-P_2O_5. In the monolithic HAp sintered body (a), the fracture mode was a typical transgranular type with a flat surface. However, a few pores less than 0.5 μm in diameter were clearly observed on the fracture surface as indicated with arrowheads. This was due to low densification. On the other hand, in the sample which contained 8 wt.% MgO-P_2O_5, intergranular and transgranular fracture modes were observed with rough and flat surfaces.

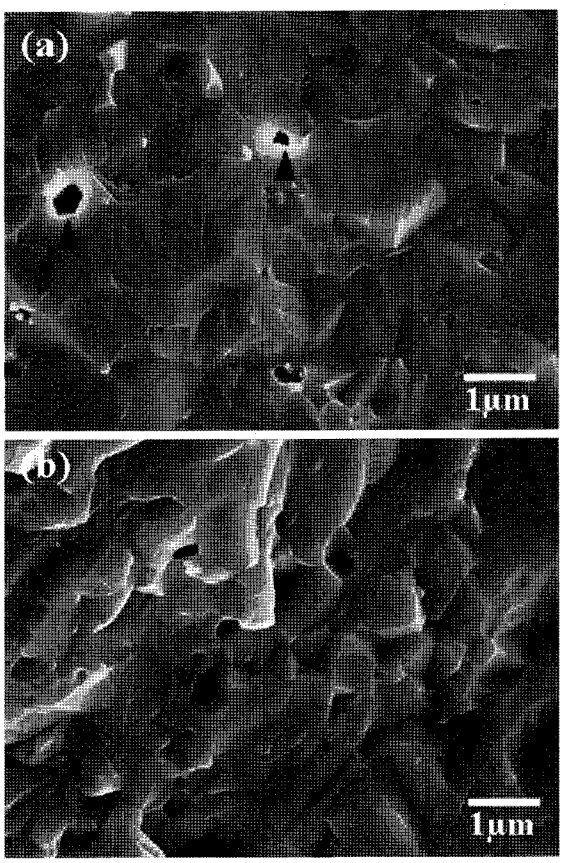

Fig. 6. SEM fracture surfaces of HAp sintered bodies depending on MgO-P_2O_5 content; (a) 0 wt.% and (b) 8 wt.%.

Fig. 7 shows osteoblast cells grown on the HAp sintered bodies which contained (a) 0 wt.%, (b) 4 wt.% and (c) 8 wt.% MgO-P_2O_5. Fig. 7(d), (e) and (f) are enlarged images of (a), (b) and (c), respectively. To understand how well osteoblast cells attach, anchor and proliferate on the sintered bodies, the SEM characterizations were conducted

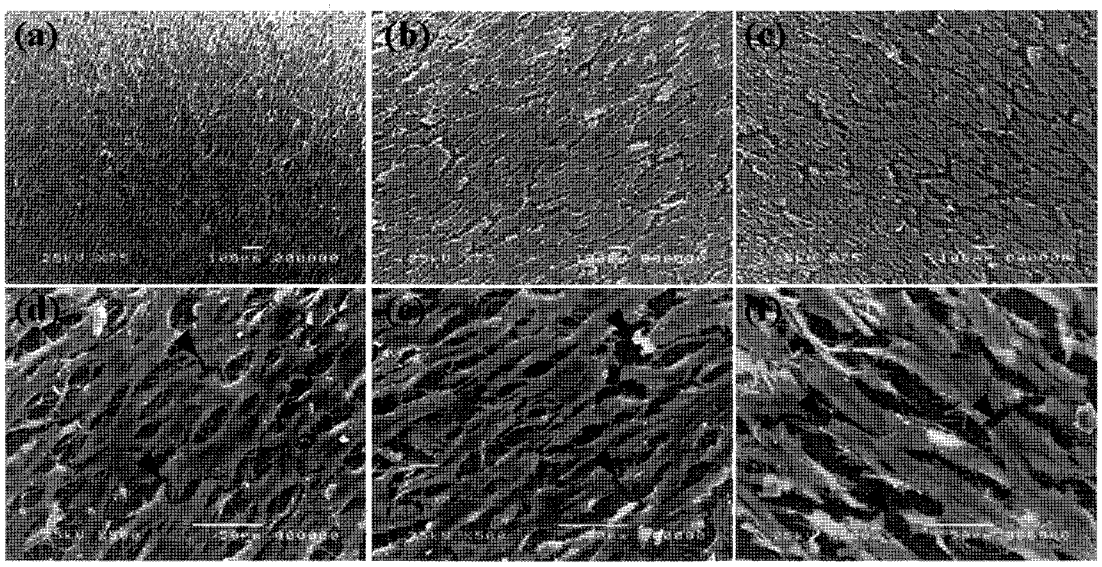

Fig. 7. SEM micrographs of osteoblast cells grown on HAp sintered bodies depending on MgO-P_2O_5 content; (a, d) 0 wt.%, (b, e) 4 wt.% and (c, f) 8 wt.%.

on monolithic HAp, and 4 and 8 wt.% $MgO-P_2O_5$ contained HAp sintered bodies cultured with osteoblast cells for 5 days. From SEM observation, it was clear that the spindle shape osteoblast cells were well grown, and had spread well on the surface, and fully covered the ceramic matrices as shown in Fig. 7(a), (b) and (c). In the enlarged images shown in Fig. 7(d), (e) and (f), it was confirmed that the growth behaviors of osteoblast cells grown on the monolithic HAp, and 4 and 8 wt.% $MgO-P_2O_5$ content HAp sintered bodies were almost the same. The arrowheads in the pictures indicate that the cells were artificially cut during the procedure of sample preparations for SEM.

Fig. 8 shows osteoclast cells grown on the HAp sintered bodies which contained (a, d) 0 wt.%, (b, e) 4 wt.% and (c, f) 8 wt.% $MgO-P_2O_5$. From the SEM images, it was found that the osteoclast cells grown on the monolithic HAp, and 4 and 8 wt.% $MgO-P_2O_5$ content HAp sintered bodies showed similar findings. In all samples, the cells were fully covered and spread well on the surface of the sintered bodies within 5 days. The cells directly anchored on sintered bodies with spindle shapes, and lots of grape like round osteoclasts with many fine processes were found on the spindle shaped osteoclasts as shown in Fig. 8(d, e, f).

4. Conclusions

The material properties such as density, Vickers hardness and fracture toughness of hydroxyapatite (HAp) ceramic were improved significantly by adding a small quantity of $MgO-P_2O_5$ based sintering additive. As the sintering additive was increased to over 4 wt.%, the few amount of HAp phase was decomposed and transformed to β-TCP. In the case of monolithic HAp sintered bodies, the material properties such as density, hardness and fracture toughness were comparatively lower than those of other samples due to contain a few pores. The density, Vickers hardness and fracture toughness of HAp sintered bodies which contained 0 and 2 wt.% $MgO-P_2O_5$ were about 2.83 gm/cc, 425 Hv and 3.10 gm/cc, 657 Hv, respectively. But, the maximum fracture toughness that was found in 8 wt.% $MgO-P_2O_5$ content sample was about 1.02 $MPa \cdot m^{1/2}$ due to the volume increase that accompanies the transformation of HAp to β-TCP phase.

From the in-vitro study, both types of human osteoblast-like MG-63 cells and osteoclast raw 264.7 cells grew well on the monolithic HAp, and 4 and 8 wt.% $MgO-P_2O_5$ content HAp sintered bodies and fully covered them within 5 days. The cells were spindle shape in osteoblasts and spindle shaped or had a grape- like appearance in osteoclasts.

Acknowledgement

This work was supported by NRL research program of the Korean Ministry of Science and Technology.

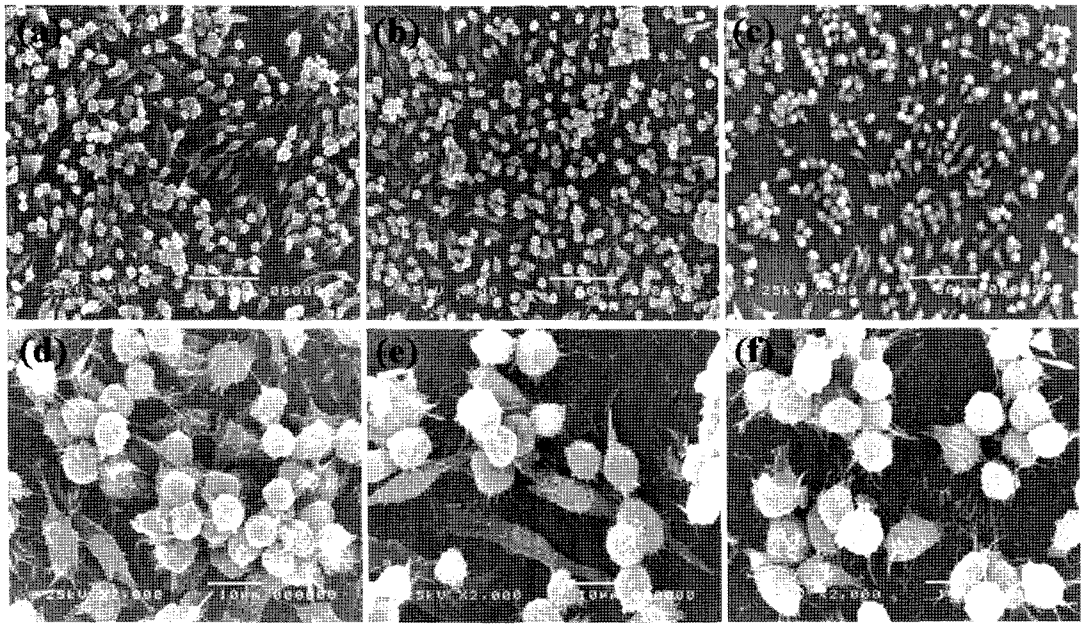

Fig. 8. SEM micrographs of osteoclast cells grown on HAp sintered bodies depending on $MgO-P_2O_5$ content; (a, d) 0 wt.%, (b, e) 4 wt.% and (c, f) 8 wt.%.

References

1. F. Watari, A. Yokoyama, F. Saso, M. Uo and T. Kawasaki, Comp. Part B, **28B**, 5 (1997).
2. P. Ducheyne and Q. Qiu, Biomaterials, **20**, 2287 (1999).
3. L. L. Hench, J. Am. Ceram. Soc., **74**, 1487 (1991).
4. L. L. Hench, J. Am. Ceram. Soc., **81**, 1705 (1998).
5. R. Z. Legeros, S. Lin, R. Rohanizadeh, D. Mijares and J. P. Legeros, J. Mater. Sci. Mater. Med., **14**, 201 (2003).
6. S. J. Kalita, S. Bose, H. L. Hosick and A. Bandopadhya, Biomaterials, **25**, 2331 (2004).
7. C. Ribeiro, E. C. S. Rigo, P. Sepulveda, J. C. Bresslani and A. H. A. Bresslani, Mater. Sci. Eng., **C 24**, 631 (2004).
8. K. J. L. Burg, S. Porter and J. F. Kellam, Biomaterials, **21**, 2347 (2000).
9. A. K. Dash and G. C. Cudworth, J. Pharmacol. Toxicol. Method, **40**, 1 (1998).
10. W. Suchanek and M. Yoshimura, J. Mater. Res., **13**, 94 (1998).
11. E. Adolfsson, P. Alberiushenning and L. Hermansson, J. Am. Ceram. Soc., **83**, 2798 (2000).
12. M. A. Lopes, F. J. Monteiro and J. D. Santos, Biomaterials, **20**, 2085 (1999).
13. J. D. Santos, J. C. Knowles, R. L. Reis, F. J. Monteiro and G. W. Hastindgs, Biomaterials, **15**, 5 (1994).
14. J. C. Knowless, S. Talal and J. D. Santos, Biomaterials, **17**, 1437 (1996).